Phys Chem Minerals (1987) 14:2–12

PHYSICS AND CHEMISTRY OF MINERALS


# Theoretical Study of the Structure, Lattice Dynamics, and Equations of State of Perovskite-type $MgSiO_3$ and $CaSiO_3$

R.J. Hemley[1], M.D. Jackson[2]*, and R.G. Gordon[2]

[1] Geophysical Laboratory, Carnegie Institution of Washington, Washington, D.C. 20008, USA
[2] Department of Chemistry, Harvard University, Cambridge, Massachusetts 02138, USA

**Abstract.** The structural distortions, lattice dynamics, and equations of state of the high-pressure perovskite phases of $MgSiO_3$ and $CaSiO_3$ are examined with a parameter-free theoretical model. A theoretical ionic description of the crystal charge density is constructed from shell-stabilized ions, whose wavefunctions are calculated from Hartree-Fock theory. The short-range forces are then calculated in the pairwise-additive approximation from modified electron gas theory. The resulting many-body-corrected pair potentials are used to study the lattice dynamics in the quasiharmonic approximation. The cubic structure of $MgSiO_3$ perovskite (*Pm3m*) is found to be dynamically unstable at all pressures, with imaginary quasiharmonic phonons occurring at the edge of the Brillouin zone. In contrast, the cubic phase of $CaSiO_3$ perovskite is found to be stable at low pressures but becomes dynamically unstable at $\sim 109$ GPa (1.09 Mbar). Energy minimization of $MgSiO_3$ in an orthorhombic cell (*Pbnm*) is performed to obtain a distorted perovskite structure that is dynamically stable. The calculated unit cell parameters at zero pressure and room temperature are within 2 percent of those determined by x-ray diffraction. The theoretical equation-of-state calculations predict a lower compressibility and thermal expansivity for the two silicate perovskites than does the available experimental data on these compounds. Extensions of the present ionic model for more accurate predictions will require the inclusion of polarization of charge density and vibrational anharmonicity.

## I. Introduction

The possibility that silicates may adopt the extremely dense perovskite structure at very high pressures was originally suggested by Ringwood (1962). Silicate perovskite phases of various compositions were subsequently synthesized in high-pressure laboratory studies (Ringwood and Major 1967, 1971, Liu 1974, Liu and Ringwood 1975, Ito and Matsui 1978, 1979, Yagi et al. 1978, 1982). Densities measured for the perovskite-type $MgSiO_3$ and $CaSiO_3$ were found to be the largest of any known silicate phases. On the basis of these results, it has been widely assumed that the lower mantle may be composed of such compounds (see Jeanloz and Thompson 1983). Because these phases may dominate the mineralogy of this region of the earth's interior, their material properties at high pressures and temperatures are of considerable geophysical importance.

Despite the importance of the silicate perovskites for earth science, useful experimental data under geophysically relevant conditions are generally lacking. Synthesis of crystals of sufficient quality for the study of material properties has proven difficult. The $MgSiO_3$ perovskite has been studied, however, by powder x-ray diffraction at 1 bar and to pressures of 8.5 GPa (85 kbar), from which unit-cell parameters and compressibility have been obtained (Yagi et al. 1982). The results of electron transmission microscopy of that sample have been interpreted to indicate a superstructure based on the structure indexed for the x-ray refinement (Madon et al. 1980). Some information on the phonon properties is available from a measurement of the infrared spectrum (Weng et al. 1983), but the observed bands are not well resolved and have not been assigned. Recently, the thermal expansivity of $(Mg_{0.9}Fe_{0.1})SiO_3$ was measured to $\sim 800$ K at 1 bar (Knittle et al. 1986), but there is, as yet, no direct information on the variation of thermal expansion with pressure. Even less is known about the properties of perovskite-type $CaSiO_3$. Ringwood and Major (1967, 1971) successfully synthesized perovskite forms of $CaSiO_3$ in solid solution with $CaGeO_3$. Liu and Ringwood (1975) later synthesized the end-member phase and obtained an x-ray diffraction pattern at high pressure (16.0 GPa) that was indexed as cubic. The phase could not be quenched to 1 bar, in contrast to the behavior of $MgSiO_3$-perovskite.

In addition to their importance to solid-earth geophysics, the silicate perovskites provide further examples with which to examine details of the crystal chemistry of the general class of perovskite materials. As discussed by Glazer (1972, 1975), a number of distortions from the ideal cubic perovskite structure is possible (Fig. 1). This behavior may be controlled in part by the relative sizes of the A and B cations and X anions in these $ABX_3$ compounds (Yagi et al. 1978). The $MgSiO_3$ perovskite represents one extreme in this regard, with the small radius of the A cation (Shannon and Prewitt 1969). In $CaSiO_3$, the radius of the cation in the A site is significantly larger. Therefore, on the basis of simple radius ratio arguments, one should except larger distortion in the magnesium than in the calcium perovskite. The extent to which these simple ionic radius ratio arguments are valid is examined in the present study.

* *Present Address*: Department of Geological Sciences, Virginia Polytechnic Institute and State University, Blacksburg, Virginia 24061, USA

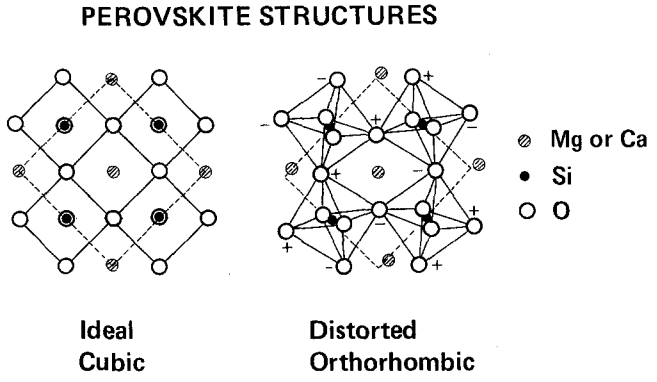


**Fig. 1.** Ideal cubic and distorted perovskite structures (from Megaw 1973)

In order to provide quantitative predictions for the material properties of the silicate perovskites as well as to provide a more complete understanding of the observed behavior at the atomic level, these phases are examined in the present paper with a theoretical, parameter-free model (Hemley et al. 1985a, b). The model is based on an electron-gas treatment of the interatomic interactions (Gordon and Kim 1972, Waldman and Gordon 1979). Although the pairwise-additive approximation is used in this approach, many-body contributions are incorporated in the interatomic pair potentials in a self-consistent manner (Hemley and Gordon 1985). The energy-minimized structures for the two perovskites are determined. This procedure is essential for a quantitative analysis of these crystals because of the possibility of large deviations from the ideal, cubic structure. Lattice dynamics calculations are performed with a modified rigid-ion, quasiharmonic approximation (Born and Huang 1954). The calculations provide further insight into the distortion mechanism and provide theoretical estimates of the phonon properties, which can be compared with available experimental data. From a converged calculation of the quasiharmonic phonon frequencies as a function of wavevector, the quasiharmonic vibrational free-energy and thermal expansivity of the crystals are calculated.

## II. Method

*Static Energy and Structure*

The procedures used for calculating the static and lattice-dynamical properties of the crystal are outlined in this section. A more detailed and general description of the method for treating the static energy is given by Muhlhausen and Gordon (1981a). A perfect crystal is assumed. As described previously (Hemley and Gordon 1985), the total charge density is written as a superposition of the component ion densities expressed as

$$\rho_T(x)=\sum_i \sum_l Z_i\,\delta(x-r_{il})-\rho_i(x-r_{il}) \tag{1}$$

where $\rho(x-r_{il})$ is the electron density of an ion centered at $r_{il}$, $Z_i$ is the nuclear charge, and $\delta$ is a delta function. The summations include all ions $i$ of the unit cell and lattice vectors $l$. The binding energy of the crystal $U_B$ is defined as the crystal interaction energy per formula unit relative to the fixed charge densities $Z_i\delta(x)-\rho_i(x)$ at infinite separation. The energy has contributions from electrostatic, kinetic, exchange, and correlation terms. The electrostatic interaction energy (per unit cell) is given by

$$U_E=1/2\int dx \sum_i [Z_i\delta(x-r_i)-\rho_i(x-r_i)\,\Phi_i(x), \tag{2}$$

where

$$\Phi_i(x)=\int dx' [\rho_T(x')-Z_i\,\delta(x'-r_{il})+\rho_i(x'-r_{il})]/[x'-x].$$

The latter includes a contribution from the long-range Coulomb interaction that is calculated by the Ewald method (Ewald 1921), the exact non-point (or short-range) Coulomb interaction, and a term for the self energies of the component ions. The kinetic, exchange, and correlation energies are obtained from the energy density functionals of modified electron gas theory (MEG) (Gordon and Kim 1972, Waldman and Gordon 1979). For the perfect crystal these are obtained by integrating

$$U_\alpha=\int dx'\,\varepsilon_\alpha[\sum_i \sum_l \rho_i(x-r_{il})]-\sum_i \sum_l \varepsilon_\alpha[\rho_i(x_i-r_{il})] \tag{3}$$

for each density functional $\varepsilon_\alpha$. In the present calculations, a pairwise additive approximation is invoked, and the integrals are separated into sums of integrals over pairs of ions.

The charge densities of the ions are obtained by a Watson sphere-type calculation (Watson 1958, Muhlhausen and Gordon 1981a, b, Hemley and Gordon 1985) in which the Hartree-Fock self-consistent-field (HF-SCF) method is employed. With this technique the charge density of the ion in the crystal is simulated by placing the ion in a hollow sphere of radius $R_0$ with a charge $Q$ at the surface. The charged sphere generates a perturbing potential that is constant inside the sphere and falls off as $1/r$ outside. The difference between the HF-SCF energy with and without the perturbing field gives the ion self-energy $U_s$. A self-consistency condition is imposed to determine the choice of wavefunction for a given configuration of ions: the value of $R_0$ is fixed such that the electrostatic potential in the sphere matches the total potential at the site of the ion in the crystal. Because the site potential is a function of the configuration of ions, a series of ion shell-stabilized wavefunctions with different $R_0$ are required to determine the electrostatically self-consistent equation of state of the crystal. For the cubic structure the procedure of matching the site potential is straighforward because all of the ions of a given type are equivalent by symmetry; therefore, the site potentials for each type of ion are the same. For the distorted structures, however, the loss in symmetry results in a variation in the potential for a given type of ion in different sites in the unit cell. In this case the averaged site potential is used to match with the shell potential. The calculation was considered converged when the average value agreed with the shell potential to within 0.1 percent.

Previous MEG calculations with shell stabilized ion charge densities (SSMEG) have been performed to determine the zero-pressure properties of a number of oxide and halide crystals (Muhlhausen and Gordon 1981a, b). In these studies the shell-stabilization of charge density was found to represent the most significant many-body contribution to the calculated equilibrium properties. This result has been confirmed by more recent calculations of ionic crystals

at high pressure (Hemley and Gordon 1985, Hemley et al. 1985a, b). In the present study a series of shell-stabilized wavefunctions for $O^{-2}$ were used with $R_0$ varied over the range 0.963–1.138 Å. Because of the small size of $Mg^{+2}$, the change in $R_0$ with volume has a negligible effect on the calculated cation charge density; therefore, a single wavefunction was used. A single wavefunction was also used for $Ca^{+2}$, as the effect of varying the shell radius on the equation of state was much less than that resulting from the change in radius for the oxygen anions.

The variation in the shell radius (or potential) produces a change in the self energy of the ion with compression. The self energy is the positive shift of the ion energy that results from the shell-stabilization perturbation. For shell-stabilized $O^{-2}$ this term is calculated by the method described by Muhlhausen and Gordon (1981a). Recent work has shown that it is important to include this effect in both the calculation of the zero-pressure equilibrium structure and the equation of state (Hemley and Gordon 1985, Hemley et al. 1985b). For the case of cubic crystals studied earlier it is sufficient to calculate the lattice (or cohesive) energy as a function of the lattice constant. Numerical differentiation of the lattice energy-volume curve then gives the static pressure-volume relation. Alternatively, the calculated points can be fitted to an equation of state, such as the Eulerian finite-strain equation (Birch 1978). To calculate the crystal structure with free internal parameters one must minimize the static energy at zero-pressure or the Gibbs free energy, $G=E+PV$, under applied pressure.

In the present calculations of the distorted perovskite phases two procedures were examined. The Gibbs free energy (minus the self-energy) was minimized at a fixed pressure with a set of pair potentials calculated with a given shell radius on the oxygen anions. The pressure was then varied to satisfy the site potential matching criterion described above. The static energy plus the appropriate self energy was then fitted with a fourth-order Eulerian finite-strain expansion (Hemley and Gordon 1985). The second procedure involves constructing from the minimization results a single, structure-dependent, pair potential for each interaction together with a function representing the dependence of the self energy on the site potential (Jackson 1986). The compiled potential was obtained by determining the nearest neighbor M–O, Si–O, and O–O distances for each volume and concatenating the corresponding points from each pair potential. The final set of points then provides a crystal-potential (i.e., many-body) corrected, pair potential that is valid over the range of compression studied. With a set of compiled pair potentials, the zero-pressure unit-cell parameter for cubic $MgSiO_3$ in the static lattice limit was found to be within 0.1 percent of that determined by the first method. For the lattice-dynamical calculations, however, the compiled potentials required considerable smoothing or fitting to a prescribed functional form in order to avoid spurious oscillations in quasiharmonic frequencies and vibrational free energy. Because of this problem, the first procedure described above was used in the present study.

*Lattice Dynamics and Equations of State*

The lattice-dynamics calculation was performed in the quasiharmonic approximation, according to which the crystal potential is expanded to second order at a given value of the lattice constant (Born and Huang 1954). This approximation generates volume-dependent phonon frequencies, $\nu_i(V)$. The usual periodic boundary conditions are imposed in order to determine the elements of the dynamical matrix (Born and Huang 1954). The matrix elements are obtained from the first and second derivatives of the Madelung and short-range parts of the SSMEG pair potentials. The quasiharmonic phonon frequencies $\nu_i(V)$ are determined by diagonalization of the dynamical matrix for a given wavevector $k$. In the present treatment, the rigid-ion approximation is assumed for each value of the lattice constant, and the dynamical contribution from shell stabilization is neglected (e.g., Boyer et al. 1985). The derivatives of the pair potentials were obtained by cubic spline interpolation of the tabulated SSMEG curves.

In the quasiharmonic approximation, the Helmholz free energy of the crystal can be written (Born and Huang 1954)

$$F(V,T)=U(V)+1/2\sum_i h\nu_i(V) + k_BT\sum_i \ln(1-\exp[-h\nu_i(V)/k_BT]). \quad (4)$$

where $T$ is the temperature, $h$ is Planck's constant, and $k_B$ is Boltzmann's constant. The summation formally includes all the normal modes in the crystal at a given $V$. For the cubic case, a grid of $\sim$1,000 points in the Brillouin zone was used. For the distorted structures with their larger unit cell, $\sim$150 wavevectors proved to converge adequately.

The equation of state is obtained by differentiating Eq. (4) with respect to $V$, i.e., $P=-(\partial F/\partial V)_T$. The result can be written formally in the following way,

$$P=P_E+P_{ZP}+P_{TH}. \quad (5)$$

In this expression $P$ is the externally applied pressure; $P_E$ $(=-dU_E/dV)$ is the static ground-state electronic pressure that includes a term for the self-energy pressure $(-dU_s/dV)$ due to the volume dependence of the ion self energy; $P_{ZP}$ and $P_{TH}$ are the zero-point and thermal vibrational pressures, respectively, given as

$$P_{ZP}=V^{-1}\sum_i \gamma_i h\nu_i/2 \quad (6)$$

$$P_{TH}=V^{-1}\sum_i \gamma_i h\nu_i/[\exp(h\nu_i/k_BT)-1], \quad (7)$$

where $\gamma_i$ is the mode-Gruneisen the parameter

$$\gamma_i=-\frac{d\ln\nu_i}{d\ln V}.$$

The $P-V$ isotherms [Eq. (5)] were calculated by analytic differentiation of the expression for $F(V,T)$. The Gibbs free energy as a function of both $T$ and $P$ was obtained from $G=F+PV$. Finally, the thermal Gruneisen parameter $\gamma$ and the harmonic, high-temperature Debye temperature $\Theta_{H\infty}$ were calculated from

$$\gamma=-\frac{d\langle\ln\omega\rangle}{d\ln V} \quad (9)$$

and

$$\Theta_{H\infty}=\frac{h}{2\pi k}\left(\frac{5}{3}\right)^{1/2}\langle\omega^2\rangle, \quad (10)$$

where $\langle\ln\omega\rangle$ and $\langle\omega^2\rangle$ are averages over the quasiharmonic frequency spectrum (Wallace 1972).

**Table 1.** Bond lengths and dissociation energy of cubic $MgSiO_3$ and $CaSiO_3$ perovskite[a]

| | MEG[b] | SSMEG[c] | SSMEG[d] |
|---|---|---|---|
| $MgSiO_3$ | | | |
| Si–O (a/2) | 1.88 Å | – | 1.742 Å |
| Mg–O, O–O ($\sqrt{2}$a/2) | 2.66 Å | – | 2.464 Å |
| $D_e$, eV/molecule | – | – | 143.6 |
| $CaSiO_3$ | | | |
| Si–O (a/2) | 1.91 Å | 1.790 Å | 1.784 Å |
| Ca–O, O–O ($\sqrt{2}$a/2) | 2.70 Å | 2.531 Å | 2.523 Å |
| $D_e$, eV/molecule | – | 141.7 | 141.0 |

[a] Zero-pressure, static-lattice calculation; $a$ is the lattice constant, and $D_e$ is the dissociation energy required to separate the crystal into gas-phase ions

[b] Wolf and Jeanloz (1985); modified electron gas calculation with a Watson sphere model with charge of +1 for the oxygen anion

[c] Muhlhausen and Gordon (1981b); many-body overlap terms were evaluated explicitly in this calculation; correction factors for 28 electrons as in the present work were used

[d] This work

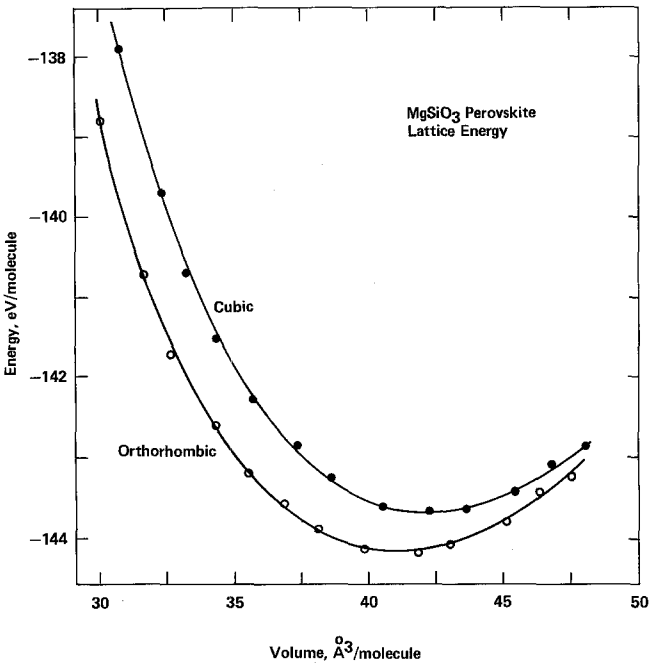


**Fig. 2.** Volume dependence of the static-lattice energy of $MgSiO_3$ perovskite

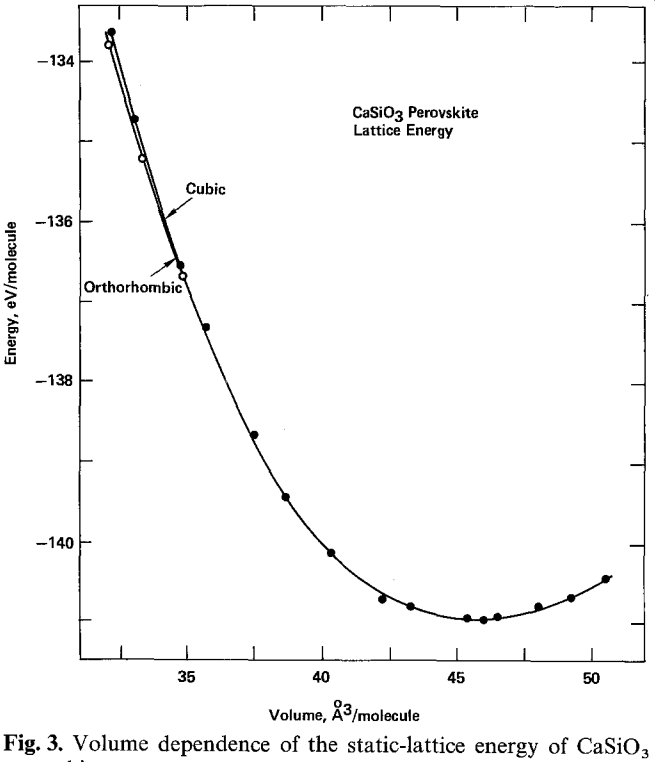


**Fig. 3.** Volume dependence of the static-lattice energy of $CaSiO_3$ perovskite

## III. Results

*Cubic Perovskites: Static Lattice*

The results of the static-lattice calculation (no thermal contribution) are considered first. The calculated structures and dissociation energies for the cubic perovskite polymorphs of $MgSiO_3$ and $CaSiO_3$ at zero pressure are detailed in Table 1. These coordinates correspond to the minimum of the lattice energy-volume curves for the cubic structures, as shown in Figures 2 and 3. For the cubic crystal, all bond lengths are given by one parameter each (e.g., lattice parameter $a$). The results of a MEG calculation performed concurrently by Wolf and Jeanloz (1985) are also listed. In their calculation the oxygen charge density was determined from a Watson sphere model with a charge of +1 and a fixed radius of $R_0 = 1.408$ Å (Watson 1958, Cohen and Gordon 1976), whereas in the present calculation a charge of +2 was used and the shell radius was varied to maintain electrostatic self-consistency. It is apparent from the results listed for the two calculations that the form of the shell potential used for the calculation of the oxygen charge density by a Watson sphere-type model has a pronounced effect on the calculated structure. This result has been demonstrated previously for numerous other oxide crystals (Muhlhausen and Gordon 1981a, b, Hemley et al. 1985b).

For $CaSiO_3$ the results of a full many-body calculation carried out by Muhlhausen and Gordon (1981b) are also compared in Table 1. The method employed by Muhlhausen and Gordon (1981b) is similar to that employed here in that self-consistent, shell-stabilized ions were used. In the previous calculation, however, the many-body contribution arising from the overlap of charge density from three or more ions was included (although the effect of volume dependence of the ion self energy was not included in determining the minimum energy structure). The results of the two calculations are similar. The agreement suggests that the pairwise calculation with the effective many-body corrected pair potentials provides a useful approximation for further calculations, including those required for lattice dynamics and equations of state (Hemley and Gordon 1985).

*Lattice Dynamics of Cubic Perovskites*

Although the minimum energy configuration of the ions can be easily determined (especially for a cubic crystal), one

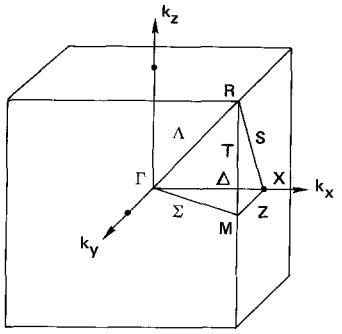


**Fig. 4.** First Brillouin zone for the cubic perovskite crystal

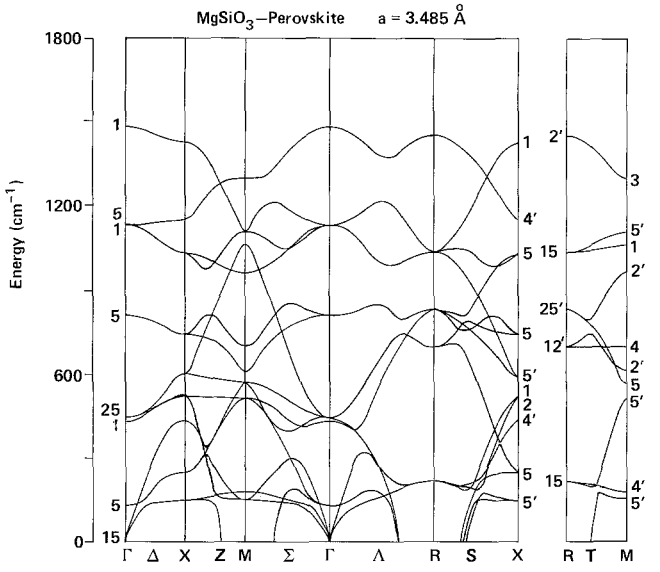


**Fig. 5.** Phonon dispersion relations for $MgSiO_3$ perovskite at the minimum energy configuration for the cubic structure for the static lattice at zero pressure

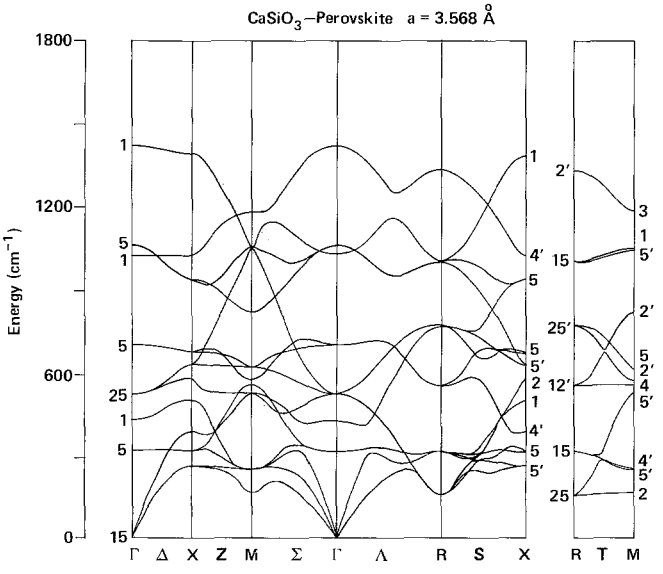


**Fig. 6.** Phonon dispersion relations for cubic $CaSiO_3$ perovskite at the static-lattice, zero-pressure energy minimum

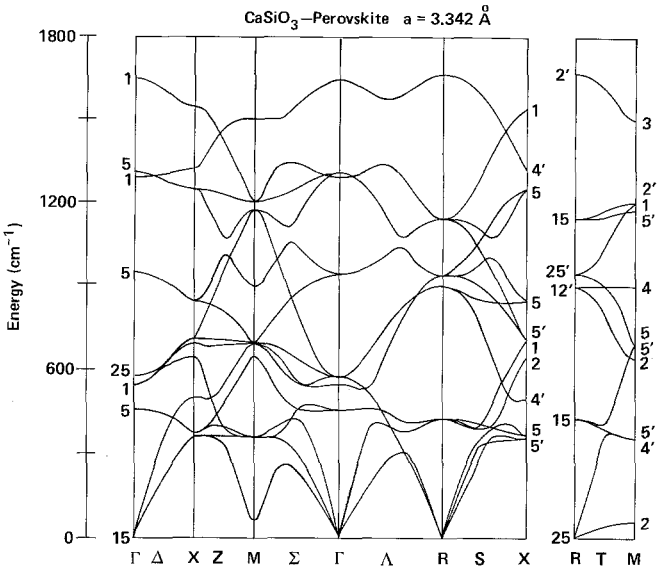


**Fig. 7.** Phonon dispersion relations for $CaSiO_3$ perovskite at the high-pressure $R$-point instability in the cubic structure

must evaluate the second derivatives of the crystal potential with respect to displacements of the component ions in order to determine whether the calculated minimum energy structure is in fact dynamically stable. A dynamical instability will obtain if the configuration of ions exists on a saddle point of the crystal potential. Dynamical instabilities are evident as imaginary frequencies in the quasiharmonic mode spectrum. The magnitude of the imaginary component indicates the degree of negative curvature of the potential along that coordinate in the crystal (i.e., the degree of instability).

The first Brillouin zone for a simple cubic crystal is shown in Figure 4. The labelling of the points follows the convention of Bouckaert et al. (1936). In Figure 5 the calculated dispersion of the quasiharmonic frequencies in the Brillouin zone for cubic $MgSiO_3$ at the static-lattice energy minimum is shown ($a = 3.485$ Å). The symmetry designations of the various branches were made by comparing the calculated eigenvectors with those published by Cowley (1964) (see also Boyer and Hardy 1981). Instabilities are calculated to occur along $\Sigma$, $\Lambda$, $S$, and $T$. The unstable modes have a maximum imaginary frequency at the $R$- and $M$-points at the edge of the Brillouin zone, and are designated $R_{25}$ and $M_2$, respectively. It is noted that the entire branch along $T$ (from $R_{25}$ to $M_2$, designated $T_2$) is imaginary.

The unstable modes have eigenvectors that involve motion of the oxygen ions and may be viewed as coupled librational modes of the $SiO_6$ octahedra. The $R_{25}$ mode involves alternating in-phase and out-of-phase rotation of adjacent (corner-sharing) octahedra in successive planes in the crystal. The $M_2$ mode corresponds to in-phase rotation of $SiO_6$ groups along one axis and out-of-phase motion of polyhedra along the other two orthogonal axes. That these modes are unstable in the cubic structure means that a lower energy minimum exists at some point along one of these coordinates – that is, in a distorted perovskite structure. Significantly, this distortion is found to occur for all values of unit-cell constant, as discussed below.

**Table 2.** Equilibrium structure of $CaSiO_3$ perovskite: cubic, *Pm3m* ($Z=1$)

| | SSMEG[a] | Exp.[b] |
|---|---|---|
| $V$(unit cell) | 45.81 Å$^3$ (43.95 Å$^3$) | – (42.36 Å$^3$) |
| Si–O (a/2) | 1.789 Å (1.765 Å) | – (1.743 Å) |
| Ca–O, O–O ($\sqrt{2}$a/2) | 2.530 Å (2.495 Å) | – (2.465 Å) |

[a] The top line gives the calculated result for $P=0$, $T=298$ K. For comparison with the experimental result, the theoretical prediction for 16.0 GPa and $T=298$ K is given in parentheses
[b] Liu and Ringwood (1975); $P=16.0$ GPa and room temperature

Further insight into this behavior in $MgSiO_3$ is gained by comparing the results for $CaSiO_3$, also in the cubic structure. The dispersion relations for $CaSiO_3$ at the equilibrium static-lattice configuration ($a=3.568$ Å) are shown in Figure 6. In this case, the quasiharmonic mode spectrum has no imaginary components, and in particular, the $T_2$ branch is now found to be stable. On the other hand, the branches that were found to be unstable in cubic $MgSiO_3$ soften on compression of the structure. At $a=3.342$ Å, the instability in the $R_{25}$ mode is reached, as shown in Figure 7. The $M_2$ mode is still stable at this value of the unit cell constant but becomes unstable on further compression. The pressure at which the dynamical instability occurs is 109 GPa (298 K).

According to the present calculation, therefore, the cubic form of $CaSiO_3$ perovskite below ~100 GPa (1.0 Mbar) is stable relative to the lower symmetry distortions described above. This result is in agreement with the available experimental data on $CaSiO_3$ perovskite. The structural parameters for cubic $CaSiO_3$, including the thermal correction for 298 K calculated from the lattice dynamics, are listed in Table 2. The results for 16.0 GPa are also listed for comparison with experiment. The calculated bond lengths are close to those determined from the *in situ* x-ray measurement, with the theoretical results being 1.3 percent larger.

### *Distorted Perovskites*

The fact that dynamical instabilities are found for $MgSiO_3$ in the cubic perovskite structure implies that the coordinates must be relaxed in a more extensive energy minimization procedure to obtain the true static-lattice equilibrium structure from the model. The minimization was carried out for the orthorhombic structure with space group *Pbnm*, also known as the $GdFeO_3$ structure (Wyckoff 1964). This structure has ten parameters (three lattice and seven internal positional parameters). As mentioned above, the calculation was performed by minimizing the Gibbs free energy to obtain a structure in which the average site potential of the oxygens ions matched the shell potential used for the original calculation of the pair potentials. The volume dependence of the static-lattice energy for $MgSiO_3$ in the orthorhombic modification is compared with the cubic case in Figure 2. The orthorhombic structure is found to be more stable for all volumes, with 0.483 eV/molecule between minima.

**Table 3.** Zero-pressure equilibrium structure of $MgSiO_3$ perovskite: orthorhombic, *Pbnm* ($Z=4$)

| | SSMEG[a] | Exp.[b] |
|---|---|---|
| $V$(unit cell) | 166.60 Å$^3$ | 162.75 Å$^3$ |
| a | 4.849 Å | 4.780(1) Å |
| b | 4.937 Å | 4.933(1) Å |
| c | 6.959 Å | 6.902(1) Å |
| Mg x | 0.995 | 0.974(7) |
| Mg y | 0.020 | 0.063(5) |
| Mg z | 1/4 | 1/4 |
| 0(1) x | 0.080 | 0.096(10) |
| 0(1) y | 0.480 | 0.477(11) |
| 0(1) z | 1/4 | 1/4 |
| 0(2) x | 0.711 | 0.696(7) |
| 0(2) y | 0.288 | 0.291(7) |
| 0(2) z | 0.042 | 0.056(4) |
| Si–O(1) | 1.784 Å | 1.79(1) Å |
| Si–O(2) | 1.770 Å | 1.75(3) Å |
| Si–O(2) | 1.771 Å | 1.82(3) Å |
| Mean Si–O | 1.775 Å | 1.79 Å |
| Mg–O(1) | 2.073 Å | 2.10(6) Å |
| Mg–O(1) | 2.309 Å | 2.12(5) Å |
| Mg–O(2) 2x | 2.118 Å | 2.06(5) Å |
| Mg–O(2) 2x | 2.388 Å | 2.20(4) Å |
| Mg–O(2) 2x | 2.476 Å | 2.47(4) Å |
| Mg–O(1) | 2.697 Å | 2.75(6) Å |
| Mg–O(1) | 2.792 Å | 2.95(5) Å |
| Mg–O(2) 2x | 2.893 Å | 3.16(4) Å |
| Average of 6 | 2.232 Å | 2.12 Å |
| Average of 8 | 2.293 Å | 2.21 Å |
| Average of 12 | 2.468 Å | 2.48 Å |

[a] $P=0$, $T=298$ K
[b] Yagi et al. (1978); $P=0$, $T=295$ K

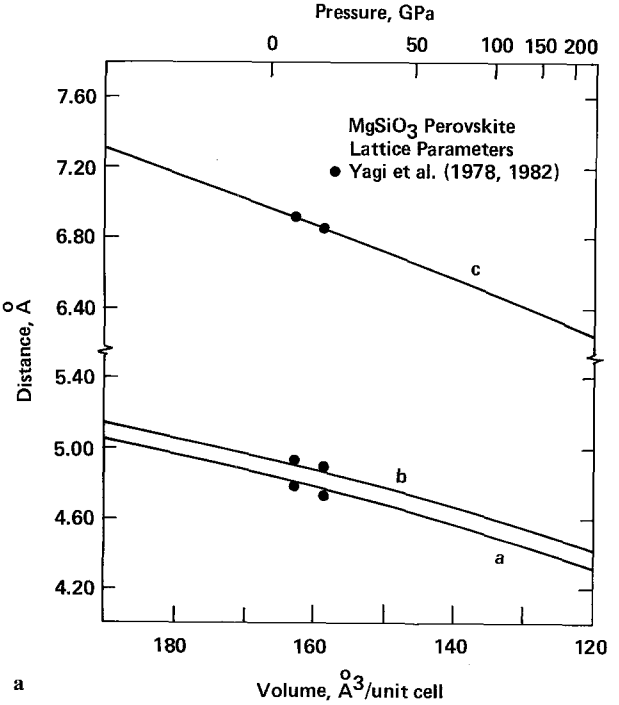


a

**Fig. 8a–c.** Volume and pressure dependence of the structure of the orthorhombic $MgSiO_3$ perovskite. (**a**) Unit-cell parameters. (**b**) Internal parameters. (**c**) Bond lengths

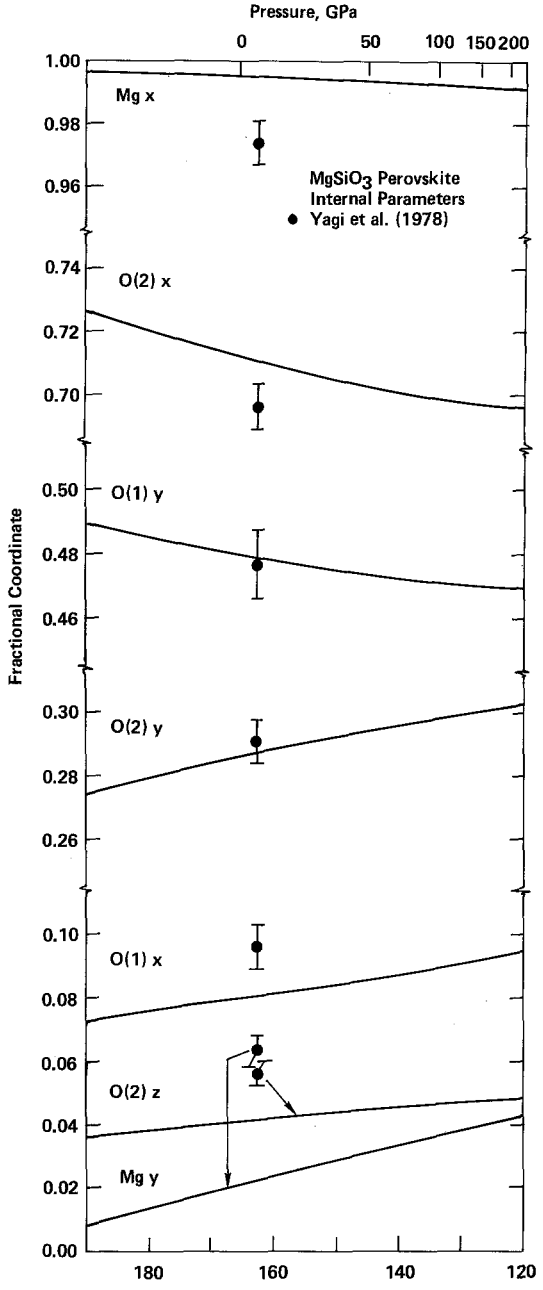


Fig. 8b

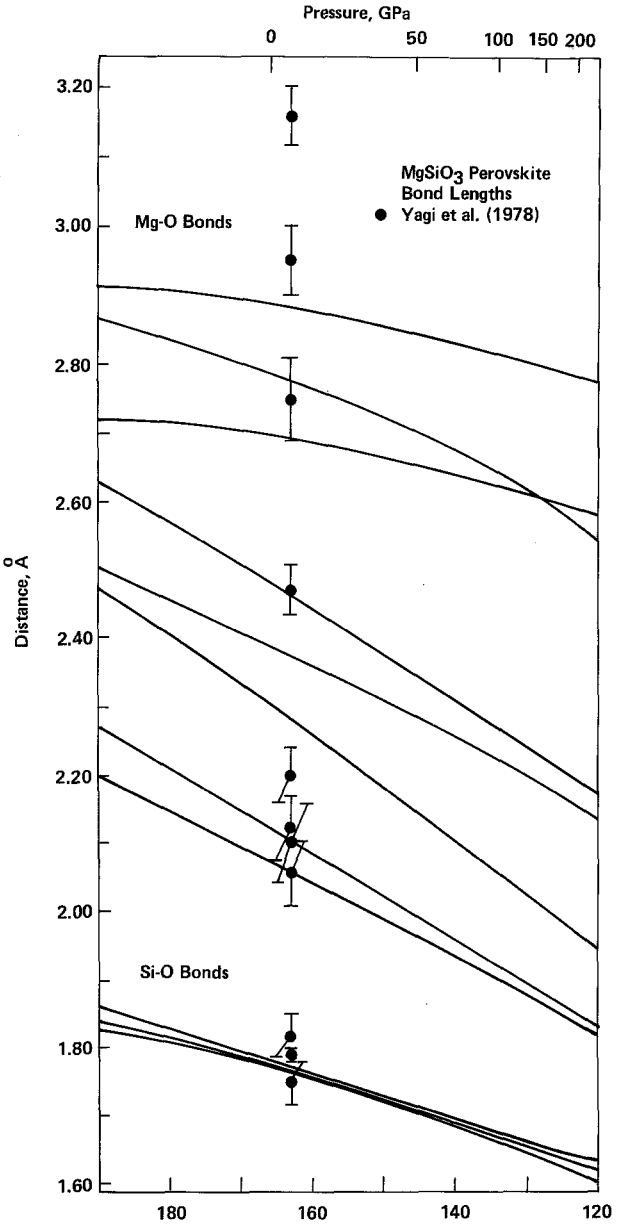


Fig. 8c

Extensive searching at low pressure for a stable distorted perovskite structure for $CaSiO_3$ failed to find one that is preferred over cubic. Interestingly, numerous local minima were found because of the small energy difference between the ideal cubic structure with no rotated octahedra and distorted forms with coupled, octahedral rotations. In each case, the ideal structure proved to be the most stable at low pressure. On compression, however, the dynamical instability occurs, as discussed above. At this point a distorted structure is favored, as shown in the splitting of the curves in the $E-V$ plot in Figure 3.

As a check on the dynamical stability of these structures, the quasiharmonic frequency spectrum for each of these structures was determined. It was found that each of these structures was indeed dynamically stable at the minimum, with real quasiharmonic frequencies. This calculation proved to be a sensitive test of the minimization near the compressional instability in $CaSiO_3$. Because of the flatness of the crystal potential with respect to octahedral rotation in this region, the energy minimization was sometimes incomplete. Incomplete minimization in turn produced weakly imaginary quasiharmonic mode frequencies in the lattice-dynamics calculation. These unstable vibrations correlate with the $R_{25}$ modes of the cubic phases; that is, they occur at the zone boundary. In the orthorhombic cell, with its quadrupled cell volume, these modes appear at zone center because of the folding in of the Brillouin zone. With the stable frequency spectrum, the thermal and zero-point contributions to the equation of state are easily determined within the quasiharmonic approximation.

The coordinates of the orthorhombic structure obtained from the minimization, including both the zero-point and

**Table 4.** Summary of equation of state parameters calculated for $MgSiO_3$ and $CaSiO_3$ perovskites[a]

| | $MgSiO_3$ | $CaSiO_3$ |
|---|---|---|
| $K_0$ (298 K), GPa | 335 (260 ± 20)[b] | 347 |
| $K'_0$ (298 K) | 0.2 | 5.3 |
| $P_{ZP,0}$, GPa | 2.77 | 2.40 |
| $P_{TH,0}$ (298 K), GPa | 0.59 | 0.45 |
| $\theta_{H\infty}$, K | 1,340 | 1,305 |
| $\gamma$ | 1.44 | 1.25 |

[a] $K_0$ and $K'_0$ are the zero-pressure bulk modulus and its pressure derivative; $P_{ZP,0}$ and $P_{TH,0}$ are the zero-point and thermal pressures at zero pressure; $\Theta_{H\infty}$ is the harmonic Debye temperature; $\gamma$ is the Gruneisen parameter

[b] Experimental results in parenthesis; Yagi et al. (1982)

thermal pressure shift for 298 K, are compared with the results of the x-ray refinement of Yagi et al. (1978) in Table 3. There is agreement between theory and experiment; in particular, the calculation reproduces the distortion in the $SiO_4$ and $MgO_{12}$ polyhedra. Although the distortions determined in the experimental structure refinement may be larger than those calculated from the model, in many cases the theoretical results are within the stated errors of the refinement. It is important to note that this refinement was based on powder-diffraction data, and is, therefore, subject to larger uncertainties than would be the case for a single-crystal study.

The question of whether the distortion in the $MgSiO_3$ perovskite will increase or decrease at pressures and temperatures characteristic of the deep mantle has been the subject of some interest in recent literature (e.g., Yagi et al. 1978, 1982). The problem has not been resolved because structural studies at high pressure have not been performed above 8.5 GPa and temperatures other than ambient. Structural studies as a function of temperature at ambient pressure (0.1 MPa) indicate no measurable changes in the distortion (Knittle et al. 1986). The volume dependence of the parameters that describe the structure are shown in Figures 8a–c. Also shown is the corresponding pressure scale for the 298 K isotherm determined from the equation of state (see below). In agreement with experiment, the ratios of the unit-cell parameters are found to be only weakly pressure dependent. The internal positional parameters (Fig. 8b), however, do reveal an increase in the distortion from the ideal structure on compression. For example, the calculated O(2) $x$, $y$, $z$ parameters change from 0.711, 0.288, 0.042 at zero pressure to 0.696, 0.300, and 0.049 at 2 Mbar; the corresponding values for the cubic structure are 0.750, 0.250, and 0.0. A noticeable pressure dependence of the distortion in the $SiO_4$ and $MgO_{12}$ polyhedra is calculated, particularly for the latter (Fig. 8c). Most of the Mg–O bonds are calculated to be significantly more compressible than the Si–O bonds.

*Equations of State*

The calculated compression isotherms for the perovskites, including the effects of the distortion, are shown Figures 8 and 9 for $MgSiO_3$ and $CaSiO_3$, respectively. The equation of state parameters are summarized in Table 4. In Figure 9(a) the volume per unit cell for $MgSiO_3$ is plotted along with the experimental room-temperature data of Yagi et al.

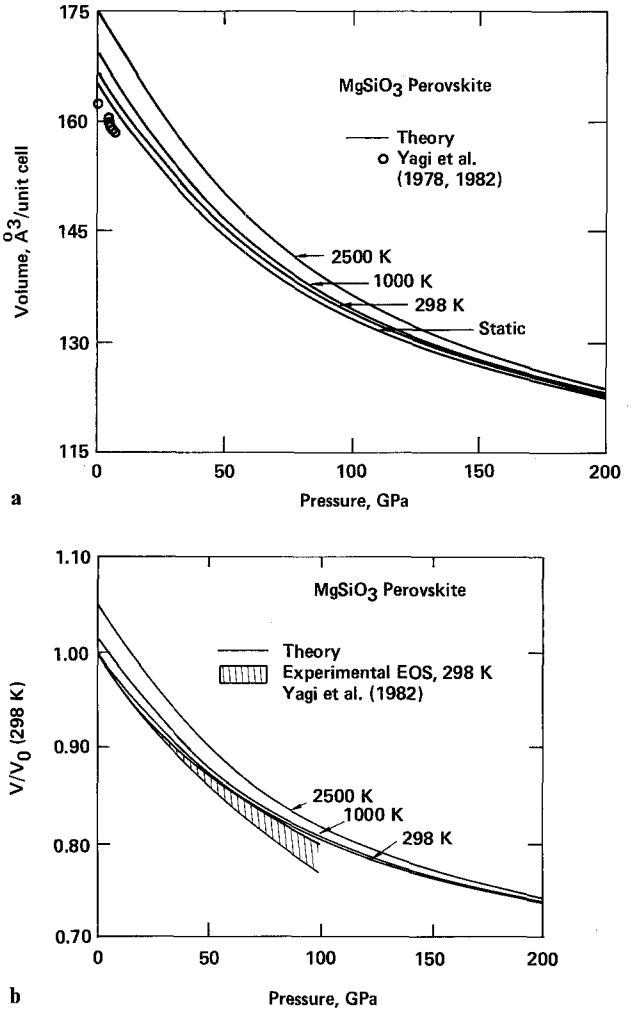


**Fig. 9a, b.** Isothermal compression of $MgSiO_3$ perovskite

(1982) to 8 GPa. An overestimation of the calculated volume (or underestimation of the pressure) relative to the experimental result is evident. The extrapolated Birch-Murnaghan equation of state determined from the experimental data is compared with the theoretical result in Figure 9(b), where the relative volume is plotted versus pressure. The envelope corresponds to the bounds on $K'_0$ that were assumed in the analysis of the data; i.e., $K'_0 = 3$ and 5 gave best fit values for $K_0$ of 262 and 255 GPa, respectively. The sum of the estimated error in the experimental bulk modulus determination ($\pm 20$ GPa) is not included in the plot (see Yagi et al. 1982).

The range of $K_0$ and $K'_0$ that was used by Yagi et al. (1982) to fit the measured points gives a more compressible crystal to megabar pressures ($\sim 100$ GPa) than the theoretical curve. At high pressure, however, the theoretical room-temperature isotherm tends to approach the upper bound obtained from the experimental analysis ($K_0 = 262$ GPa, $K'_0 = 3$). In fact, according to the calculation the pressure dependence of the bulk modulus is very weak at low pressure. This result, surprising because $K'_0 \approx 4$ for many ionic materials, is evident in the energy-volume curve in Figure 2. The volume dependence of the static energy for the distorted structure is much more symmetric about the minimum than are the curves for the cubic structures. This prediction must

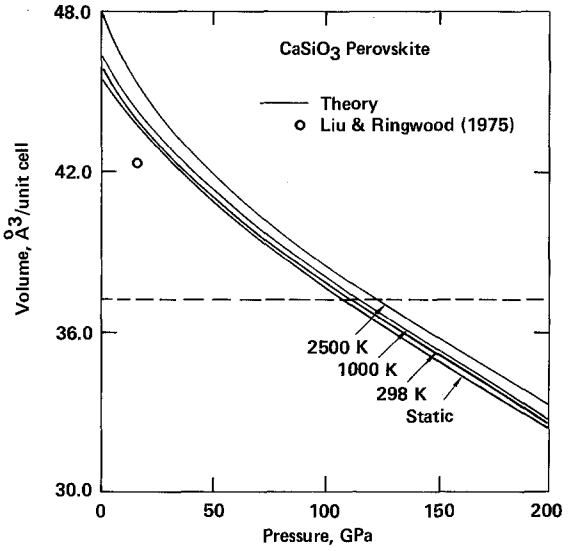


**Fig. 10.** Isothermal compression of $CaSiO_3$ perovskite. The dashed line shows the critical volume at which the cubic structure becomes unstable with respect to the $R_{25}$ phonon displacements

be tested experimentally by accurate measurements at high pressure.

For $CaSiO_3$ only one experimental point is available. This value was obtained by Liu and Ringwood (1975) using *in situ* x-ray diffraction in a diamond-anvil cell. As in the case of $MgSiO_3$, the calcium perovskite was synthesized by laser heating at high pressure, but in contrast to the former, the phase was found to be non-quenchable. The point shown in Figure 10 corresponds to 16.0 GPa. As mentioned above, the cubic phase is predicted to be stable relative to distorted tetragonal and orthorhombic phases at low pressure. The onset of the calculated distortion occurs at a volume of 37.23 $Å^3$ (109 GPa on the 298 K isotherm).

The three isotherms shown in Figures 9 and 10 illustrate the calculated pressure dependence of the thermal expansion for these two compounds. For example, for $MgSiO_3$ $\Delta V/V$ (298 K) is calculated to be 1.30 percent at 1,000 K and $P=0$. The calculated volume coefficient of thermal expansion $\alpha_V$ is $1.3\times10^{-5}$ $K^{-1}$ at 298 K, increasing to $2.1\times10^{-5}$ $K^{-1}$ at 1,000 K. The calculated thermal expansivity appears to be lower than the experimental determination to $\sim$800 K by Knittle et al. (1986) who report an average value of $4\times10^{-5}$ $K^{-1}$ at high temperature. The calculated volume change, however, is well within the error bars of the experimental study (see Knittle et al. 1986). The thermal expansivity is calculated to decrease with compression. At 1,000 K and $P=100$ GPa, $\Delta V/V$(298 K) drops by a factor of $\sim$3 to 0.45 percent. Along the 1,000 K isotherm the total vibrational pressure ($P_{ZP}+P_{TH}$) changes little, dropping from 7.70 to 7.59 GPa. The corresponding results for $CaSiO_3$ at 1,000 K are $\Delta V/V(298\,K)=1.05$ percent at $P=0$, and 0.43% at $P=100$ GPa.

## IV. Discussion

The difference in the structures obtained for the two silicate perovskites studied here can be easily explained in terms of radius ratio arguments. The cations in the $A$ site in the perovskite structure have 12-fold coordination in the ideal cubic structure. It is seen that the larger size of the $Ca^{+2}$ ion will tend to stabilize the higher symmetry structure relative to the case of the smaller $Mg^{+2}$ ion. This conclusion is identical to that of the lattice-dynamical study of Wolf and Jeanloz (1985), who employed a different set of pair potentials in their calculations. Correlations between the degree of distortion from cubic to orthorhombic and the size of the $A$ cation relative to $B$ and $O$ ions in perovskites have been studied empirically by Yagi et al. (1978). Their results are in qualitative agreement with the present non-empirical calculations.

The cubic phase of $MgSiO_3$ is dynamically unstable at all volumes (corresponding to $a=3.45$–$4.00$ Å). The triply degenerate $R$-point mode is found to be unstable, with an imaginary frequency that decreases with dilatation of the crystal. This behavior indicates that the curvature at the top of the double well corresponding to the librational coordinate drops with expansion. In the $E-V$ curve in Figure 2, one can see that energy of the orthorhombic structure does begin to approach that of cubic with increasing volume. An instability, however, in an acoustic mode (elastic instability) is reached before the curves meet. Although these results indicate that the cubic phase is not stable in terms of a quasiharmonic treatment of the phonon spectrum, it is important to realize that anharmonicities may tend to stabilize the higher symmetry structures at high temperature (i.e., first tetragonal then cubic).

It is useful to compare the results obtained for the magnesium and calcium silicate crystals studied here with calculations on halide-based perovskites by the use of similar methods. Indeed, such halide (i.e., fluoride) compounds are often used as analogues for predicting the properties of the corresponding oxides (e.g., O'Keeffe et al. 1979, O'Keeffe and Bovin 1979). Boyer and Hardy (1981) carried out a study of the zero-pressure properties of $RbCaF_3$ with a quasiharmonic lattice-dynamical model that employed (unscaled) electron-gas pair potentials. They showed that the phase transition sequence from the distorted to cubic structure can be described in terms of the loss of the double-well potential along the octahedral rotational (librational) coordinate at a critical volume that is reached on thermal expansion of the crystal. In their model for $RbCaF_3$ they found that over a temperature range of $\sim$1,000 K the thermodynamically stable state is one in which there is large amplitude motion along the librational coordinate. At a temperature of 1,200 K the double well disappears, just before the crystal develops an elastic instability that may be viewed as associated with melting. In $CsCaF_3$, on the other hand, the cubic structure was found to remain stable at all temperatures to melting (Boyer 1984, see also Flocken et al. 1985). Their result is identical to the trend observed in the present calculation for $CaSiO_3$ as a function of decreasing applied pressure. In $MgSiO_3$, however, the acoustic mode instability is reached before the librational double well is lost.

In the present calculations on the silicate perovskites, a large range of volumes was explored because of the interest in high-pressure properties of these crystals. There is a general increase in the degree of distortion for the perovskites with compression. For $MgSiO_3$ this change is perhaps most obvious in the volume dependence of the internal positional parameters (Fig. 8b). It is also apparent that the spread in bond lengths associated with the $MgO_{12}$ dodecahedron increases on compression (Fig. 8c). In contrast to these results, Yagi et al. (1978) have suggested that $MgSiO_3$

should tend toward cubic with increasing pressure. They argue that the ratio of effective ionic radii $R_A/(R_B+R_0)$ will increase because the oxygen anion is more compressible than the cations and that this will favor the cubic form at high pressure. This conclusion has been criticized by O'Keeffe et al. (1979) who propose that the pressure dependence of $(R_A+R_0)/(R_B+R_0)$, i.e., the relative bond compressibilities, controls the degree of distortion. The latter ratio decreases with compression, thus giving rise to larger tilting of $SiO_6$ octahedra and an increase in the distortion at pressure. This simple analysis is in agreement with the present theoretical result.

The calculated zero-pressure bulk modulus of $MgSiO_3$ is larger than that determined in the hydrostatic compression study of Yagi et al. (1978). The latter is close to estimates based on systematics from other perovskite-type compounds (Liebermann et al. 1977, Bass 1984). The discrepancy between these results and that of the present calculation may be indicative of the need for an improved description of the forces by the model, as discussed below. It should be pointed out, however, that values for $K_0$ and $K_0'$ are often poorly constrained by fitting compression data alone to obtain experimental equations of state. As mentioned above, the theoretical compression curve approaches the experimental equation of state at high pressure if a small value of $K_0'$ is assumed (i.e., $\sim 3$). Values for $K_0'$ of 3–6 are commonly found for ionic crystals, and such values are often assumed in fitting compression data (see Yagi et al. 1982). The present calculations suggest, on the other hand, that in highly distorted structures such as the orthorhombic perovskites, in which the internal coordinates may adjust in response to applied stresses, such systematics may break down. In this regard, there is experimental evidence that $K_0'$ for stishovite, also with 6-coordinated silicon, may be quite low (Sato 1976, see also Weidner et al. 1982). It should also be pointed out that the experimental and theoretical compression curves tend to diverge above 100 GPa. At these pressures, higher order pressure derivatives ($K_0''$) may be important in representing the experimental equation of state.

Several recent studies have addressed the question of Debye temperature $\Theta$ of $MgSiO_3$ perovskite. On the basis of empirical systematics, Watanabe (1982) estimated the thermal Debye temperature to be $1{,}204 \pm 98$ K. This result is somewhat lower than the value determined in the present study (1,340 K), which is the harmonic, high-temperature estimate $\Theta_{H\infty}$. The MEG result for $\Theta_{H\infty}$ for the cubic phase is lower (1,107 K), in part as a result of the fact that the quasiharmonic phonon spectrum has imaginary frequencies (Wolf and Jeanloz 1985). On the other hand, Knittle et al. (1986) obtained a much lower value of 525 K from a fit to the thermal expansion data (825 K for high temperature fit). Because the Debye temperature is only a crude approximation for solids with a complex distribution of lattice modes, one should expect different methods in general to give different results. Nevertheless, it is likely that the present calculations overestimate $\Theta$ because of the use of rigid-ion pair potentials (at a given volume) to calculate the lattice dynamics and the use of the quasiharmonic approximation which neglects explicit anharmonic effects. It is well known that rigid-ion models overestimate the longitudinal optic mode frequencies in ionic crystals (see Boyer et al. 1985, Hemley and Gordon 1985). Comparison with the spectrum of $MgSiO_3$ reported by Weng et al. (1983) suggests that the measured frequencies of the infrared-active modes may in fact be lower, although the spectrum is not well-resolved. The large difference between the present calculation of the Debye temperature and the value obtained from the thermal expansion measurements suggests that other factors may contribute as well; clearly, more work should be done to resolve this discrepancy. It should be pointed out that an anharmonic calculation would also be useful to test recent conjectures of fast-ion conduction (sub-lattice melting) in $MgSiO_3$ at high pressures and temperatures (O'Keeffe and Bovin 1979, Poirier et al. 1983).

Finally, extensions of the present model for the crystal potential are discussed. A significant improvement in the theory was obtained by the requirement that the shell potential used in the ion wavefunction calculation match the site potential in the crystal. The principle effect of this electrostatic self-consistency criterion in oxide crystals is the contraction of the oxygen ion wavefunction, which in turn lowers the repulsive energy of the pair potential and generally contracts the lattice. The unit-cell volumes, however, are still somewhat large, and the bulk moduli appear to be overestimated. These results are independent of the way in which the energy minimization was carried out. As discussed in Section II, an alternative procedure involving the use of pair potentials compiled from the individual potentials calculated from a fixed set of charge densities gave results that were similar to those shown here. In this study the requirement that the average site potential match the shell potential of the anions was used. An alternative formulation would be to use different charge densities, and therefore employ different sets of pair potentials, for anions in different sites. Such calculations at zero pressure, however, showed similar results to the use of single wavefunctions. Another extension would be to include the internal strain dependence of the charge densities and self energies in the energy minimization.

Perhaps the most significant discrepancies between theory and experiment are the result of the constraint that the charge densities of the ions be spherically symmetric. This notion is supported by the results obtained on $SiO_2$ polymorphs such as quartz, crystals in which an ionic model such as that used here is clearly inadequate (Jackson et al. 1985, Jackson 1986). In these crystals, the inclusion of a small degree of polarization has an important effect on the calculated unit-cell volume. The most significant effects are on the Si–O–Si bending coordinate. As the stiffness of this bending coordinate determines the magnitude of the bulk modulus, this improvement in turn produces a more accurate compression curve for quartz. A similarly stiff Si–O–Si bending potential in the distorted $MgSiO_3$ perovskite may therefore contribute to the underestimation of the degree of distortion, as well as to the overestimation of the volume and bulk modulus. In $CaSiO_3$ the inclusion of polarization would likewise lower the pressure at which the distorted structure becomes stabilized relative to the cubic aristotype. Polarization of charge density may also provide a mechanism for the stabilization of superstructures based on the $GdFeO_3$-type structure (Madon et al. 1980) and of possible ferroelectric phases of the silicate perovskites.

*Acknowledgments.* This work has benefitted from useful discussions with L.L. Boyer, H.-K. Mao, and P.M. Bell. We are grateful to L.L. Boyer for several lattice-dynamics subroutines that were adapted for the present calculations, and to A.P. Jephcoat, R.M.

Hazen, H.S. Yoder, Jr., R. Jeanloz, and an anonymous referee for reviews of the manuscript. This work was supported by grants from the National Science Foundation (EAR-8210534 and CHE-8015804).

## References


Bass JD (1984) Elasticity of single-crystal $SmAlO_3$, $GdAlO_3$, and $ScAlO_3$ perovskites. Phys Earth Planet Inter 36:145–156

Birch F (1978) Finite strain isotherm and velocities for single-crystal and polycrystalline NaCl at high pressure and 300° K. J Geophys Res 83:1257–1268

Born M, Huang K (1954) Dynamical Theory of Crystal Lattices. Oxford University Press, New York

Boyer LL, Hardy JR (1981) Theoretical study of the structural phase transition in $RbCaF_3$. Phys Rev B24:2577–2591

Boyer LL (1984) Parameter-free equation of state calculations for $CsCaF_3$. J Phys C 17:1825–1832

Boyer LL, Mehl MJ, Feldman JL, Hardy JR, Flocken JW (1985) Beyond the rigid-ion approximation with spherically symmetric ions. Phys Rev Lett 54:1940–1943

Bouckaert LP, Smoluchowski R, Wigner E (1936) Theory of Brillouin zones and symmetry properties of wave functions in crystals. Phys Rev 50:58–67

Cohen A, Gordon RG (1976) Modified electron-gas study of the stability, equilibrium structure, elastic properties, and high-pressure behavior of MgO and CaO crystals. Phys Rev B 14:4593–4605

Cowley RA (1964) Lattice dynamics and phase transitions of strontium titanite. Phys Rev 134:A981

Ewald PP (1921) The calculation of optical and electrostatic lattice potentials. Ann Phys (Leipzig) 64:253–287

Flocken JW, Guenther RA, Hardy JR, Boyer LL (1985) First-principles study of the structural instabilities in halide-based perovskites: competition between ferroelectricity and ferroelasticity. Phys Rev B 31:7252–7260

Glazer AM (1972) The classification of tilted octahedra in perovskites. Acta Crystallogr B 28:3384–3391

Glazer AM (1975) Simple ways of determining perovskite structures. Acta Crystallogr A 31:756–762

Gordon RG, Kim YS (1972) A theory for the forces between closed shell atoms and molecules. J Chem Phys 56:3122–3133

Hemley RJ, Gordon RG (1985) Theoretical study of solid NaF and NaCl at high pressures and temperatures. J Geophys Res 90:7803–7813

Hemley RJ, Jackson MD, Gordon RG (1985a) Lattice dynamics and equations of state of high-pressure mineral phases studied with electron-gas theory. Eos Transactions Am Geophys Union 66:357

Hemley RJ, Jackson MD, Gordon RG (1985b) First-principles theory for the equations of state of minerals at high pressures and temperatures: application to MgO. Geophys Res Lett 12:247–250

Ito E, Matsui Y (1978) Synthesis and crystal-chemical characterization of $MgSiO_3$ perovskite. Earth Planet Sci Lett 38:443–449

Ito E, Matsui Y (1979) High-pressure transformations in silicates, germanates, and titanates with $ABO_3$ stoichiometry. Phys Chem Minerals 4:265–273

Jackson MD (1986) Theoretical investigations of chemical bonding in minerals, Ph.D. dissertation, Harvard University

Jackson MD, Hemley RJ, Gordon RG (1985) Recent advances in electron-gas theory for minerals: self-energy corrections, charge relaxation, and bond polarization. Eos Transactions Am Geophys Union 66:357

Jeanloz R, Thompson AB (1983) Phase transitions and mantle discontinuities. Rev Geophys Space Phys 21:51–74

Knittle E, Jeanloz R, Smith G (1986) Thermal expansion of silicate perovskite and stratification of the Earth's mantle. Nature 319:214–216

Liebermann RC, Jones LEA, Ringwood AE (1977) Elasticity of aluminate, titanate, stannate, and germanate compounds with the perovskite structure. Phys Earth Planet Inter 14:165–178

Liu L-G (1974) Silicate perovskite from phase transformations of pyrope-garnet at high pressure and temperature. Geophys Res Lett 1:277–280

Liu L-G, Ringwood AE (1975) Synthesis of a perovskite-type polymorph of $CaSiO_3$. Earth Planet Sci Lett 28:209–211

Madon M, Bell PM, Mao H-K, Poirier JP (1980) Transmission electron diffraction and microscopy of synthetic high pressure $MgSiO_3$ phase with perovskite structure. Geophys Res Lett 7:629–632

Megaw H (1973) Crystal Structures: A Working Approach. Saunders, Philadelphia

Muhlhausen C, Gordon RG (1981a) Electron-gas theory of ionic crystals, including many-body effects. Phys Rev B 23:900–923

Muhlhausen C, Gordon RG (1981b) Density-functional theory for the energy of crystals: test of the ionic model. Phys Rev B 24:2147–2160

O'Keeffe M, Bovin J-O (1979) Solid electrolyte behavior of $NaMgF_3$: geophysical implications. Science 206:599–600

O'Keeffe M, Hyde BG, Bovin J-O (1979) Contribution to the crystal chemistry of orthorhombic perovskites: $MgSiO_3$ and $NaMgF_3$. Phys Chem Minerals 4:299–305

Poirier JP, Peyronneau J, Gesland JY, Brebec G (1983) Viscosity and conductivity of the lower mantle; an experimental study on a $MgSiO_3$ perovskite analogue, $KZnF_3$. Phys Earth Planet Int 32:273–287

Ringwood AE (1962) Mineralogical constitution of the deep mantle. J Geophys Res 67:4005–4010

Ringwood AE, Major A (1967) Some high-pressure transformations of geophysical significance. Earth Planet Sci Lett 2:106–110

Ringwood AE, Major A (1971) Synthesis of majorite and other high pressure garnets and perovskites. Earth Planet Sci Lett 12:411–418

Sato Y (1976) Pressure-volume relationship of stishovite under hydrostatic compression. Earth Planet Sci Lett 34:307–312

Shannon RD, Prewitt CT (1969) Effective ionic radii in oxides and fluorides. Acta Crystallogr B 25:925–946

Waldman M, Gordon RG (1979) Scaled electron-gas approximation for intermolecular forces. J Chem Phys 71:1325–1339

Wallace DC (1972) Thermodynamics of Crystals. John Wiley, New York

Watanabe H (1982) Thermochemical properties of synthetic high-pressure compounds relevant to the earth's mantle. In: Akimoto S, Manghnani MH (eds) High-Pressure Research in Geophysics. Center Acad Pub, Tokyo, pp 441–464

Watson RE (1958) Analytic Hartree-Fock solutions for $O^{--}$. Phys Rev 111:1108–1110

Weidner DJ, Bass JD, Ringwood AE, Sinclair W (1982) The single-crystal elastic moduli of stishovite. J Geophys Res 87:4740–4746

Weng K, Xu J, Mao H-K, Bell PM (1983) Preliminary Fourier-transform infrared spectra on the $SiO_6^{8-}$ octahedral group in silicate perovskite. Carnegie Inst Wash Yearb 82:355–356

Wolf GH, Jeanloz R (1985) Lattice dynamics and structural distortions of $CaSiO_3$ and $MgSiO_3$ perovskites. Geophys Res Lett 12:413–416

Wyckoff RWG (1964) Crystal Structures, Vol 2. Wiley-Interscience, New York, pp 407–412

Yagi T, Mao H-K, Bell PM (1978) Structure and crystal chemistry of perovskite-type $MgSiO_3$. Phys Chem Mineral 3:97–110

Yagi T, Mao H-K, Bell PM (1982) Hydrostatic compression of perovskite-type $MgSiO_3$. In: Saxena SK (ed) Advances in Physical Geochemistry, Vol 2. Springer-Verlag, New York, pp 317–325


Received December 5, 1985